1st Croatian Conference on Earthquake Engineering
1CroCEE
22-24 March 2021 Zagreb, Croatia

DOI: https://doi.org/10.5592/CO/1CroCEE.2021.226

Seismic behavior and design provisions for contemporary masonry chimney systems

David Antolinc[1], Vlatko Bosiljkov[2]

[1] *Teaching assistant*, University of Ljubljana, Faculty of Civil and Geodetic Engineering, *david.antolinc@fgg.uni-lj.si*
[2] *Professor*, University of Ljubljana, Faculty of Civil and Geodetic Engineering, *vlatko.bosiljkov@fgg.uni-lj.si*

Abstract

Recent events in Croatia revealed the high vulnerability of traditional unreinforced masonry chimney systems even in the case of moderate earthquakes. Chimney systems are non-structural elements and thus there is a lack of knowledge and research in this field. This topic has been in the focus of our research group through a recently finished two-stage research project oriented towards the optimization of contemporary masonry chimney systems. The main goal of the first part of the project was to experimentally identify overall behavior and main performance limits for the typical contemporary chimney systems when exposed to cyclic lateral loading. In the second part of the project, significant improvement of the behavior of the optimized system was achieved. However, since in the case of seismic loading there is significant coupling action between primary structure and non-structural elements, for the evaluation of conclusions additional numerical study was needed. It was done on detached typical masonry family house considering the floor acceleration spectra, coupling effect between primary structure and chimney, and the latest design provisions from the approaching second generation of Eurocode 8 for non-structural elements. In the end, the results are compared and discussed.

Key words: contemporary masonry chimney, non-structural element, floor acceleration spectra, earthquake

1 Introduction

Virtually all post-earthquake reconnaissance reports mention a significant number of damaged or toppled chimneys. For example, after the earthquake in New Zealand, it was reported that 14,000 chimneys were damaged or destroyed. After the Northridge earthquake for approximately 30,000 chimneys repair permits were issued in the city of Los Angeles, while other sources report a total of 60,000 damaged chimneys. Recent earthquake in Zagreb again showed high vulnerability of traditional masonry chimney systems even in the case of moderate earthquake. Beside the ornaments and knee walls, the chimneys are one of the most vulnerable elements endangering main city streets along buildings. Therefore, among the first task of the protection authority and firefighters is the removal of the building elements and material hanging above the streets. In Zagreb also a large number of volunteers from alpine club joined to remove the debris like shown in the Figure 1 from the roofs. They reported that the weakest points were chimneys, where some completely knocked down or more often semi-detached and over 600 chimneys were removed within first 20 days only by them alone [1].

Figure 1. Toppled chimney (left) and the removal of damaged and potentially hazardous chimney (right) after the Zagreb earthquake 2020 [1]

While these data reinforce the fragile nature of masonry chimneys, there are no data on the number of chimneys that were undamaged [2]. A recently completed study of the probability of exceeding a given economic loss, and damage as a function of a given seismic intensity for masonry buildings found that for low seismic events, the cost of retrofitting chimney systems can contribute significantly to the total cost of repairs for non-collapsed buildings [3]. In this study, the threshold for chimney failure was set to exceed a_g = 0.111 g [2] on the first floor of the building due to the lack of regulations. This limit could be appropriate for traditional brick masonry systems; however, it could be questionable as it concerns contemporary masonry chimney systems.

According to the new European building codes (Eurocodes) proposal prEN 1998-1-2:2019.3 (E) [4], the seismic performance of ancillary elements, that might in case of

failure, represent major hazard to persons or affect the main structure of the building or services of facilities, shall, together with their supports, be verified to resist design seismic actions [4]. The seismic analysis should be based up on the use of appropriate floor response spectra obtained from a realistic structural numerical model. The seismic action on ancillary elements can be determined as the horizontal force Fap applied to centre of mass of the ancillary element in the most unfavourable direction. The horizontal force F_{ap} is defined as:

$$F_{ap} = \gamma_a m_a S_a \tag{1}$$

Where γ_a represents the performance factor of the element, m_a the mass of the element and S_a the value in the floor acceleration spectrum.
In EN 1998-6 (EN 1998-6 2005) [5] connection specifications are given only for concrete and steel chimneys and for steel towers and guyed masts. In Informative Annex E, information and guidance for the seismic design of masonry chimneys, which are of interest for this research work, are set as:

- The behaviour factor is set as for the unreinforced masonry (q=1.5), although according to EN 1998-1, q could be set at 2.0 for chimneys that act as unreinforced cantilevers over less than half of their total height, or that are braced or braced to the structure at or above their center of mass
- Minimum vertical reinforcement - for chimneys with a horizontal dimension of up to 1 m, a total of four continuous 12 mm diameter vertical bars anchored to the foundation should be concreted between leaves of solid masonry or placed and grouted in the cells of hollow masonry units.
- Minimum horizontal reinforcement - vertical reinforcement should be enclosed within 6 mm diameter ties, or other reinforcement of equivalent cross-section at a distance not exceeding 400 mm.
- Minimum seismic anchorage should be provided at each level of floor or roof level that is more than 2 m above ground level unless it is constructed entirely within the exterior walls.
- Cantilevering - should not project from a wall or foundation as a corbel more than half the chimney wall thickness.

Whether some clauses from the Eurocode are mandatory or informative is determined by National Document for the Application (NAD) of the Eurocode. Most contemporary masonry chimney systems do not meet some of these requirements and there is a well-founded fear among chimney manufacturers that the structural requirements as set out in the informative annex of EN 1998-6 may jeopardize their position in the markets. Within this paper, we show the summary of experimental research programme for testing of contemporary masonry chimney system, which is a result of collaboration with the industrial partner, and have been presented in more extended version in [6, 7].

Those experimental results are then used to identify the damage level of the contemporary masonry chimney caused by the expected earthquake for typical modern detached family house.

2 Experimental research programme (summary)

Aware of the lack of experimental data on the lateral behaviour of contemporary masonry chimneys structurally connected to the primary structure the research program was focused on the assessment of four types of chimney systems built and tested under laboratory conditions in two phases. In the first phase, we tested two chimney systems (type A and type B) with longitudinal grouted steel reinforcement in two diagonal corners and spanning 1,5 m above and below rafters. This means that the upper 3 m of a chimney is reinforced as shown in the left Figure 3 as required by the manufacturer.
In the second phase, improved two types (type C and D) of chimneys were tested with longitudinal reinforcement spanning along with the whole height of the chimneys and fixed into the ground steel plate as shown in the right Figure 3. Type D chimney was reinforced in all four corners whereas type C was reinforced only in two diagonal corners as shown in Figure 2. For all types of tested chimneys, the same steel reinforcement ribbed bars with a diameter of 10 mm were used. The outer dimensions of light weight masonry block cross section were for all chimney types the same 36/36 cm except for the type D chimney which had dimensions of 40/40 cm.

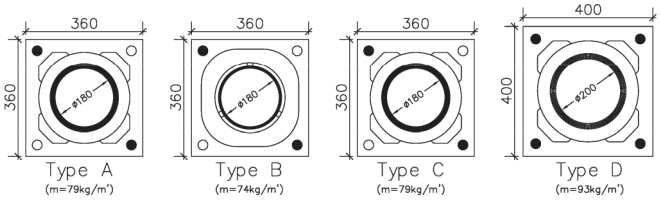

Figure 2. Horizontal cross-sections for tested types of contemporary masonry chimney systems with characteristics for light-weight concrete masonry units and overall weight of the system (dimension units are in mm)

The main objectives of this study were set as follows:

- Identification of failure mechanisms. The conservative approach to the design of chimney systems is to consider them as cantilevered systems from the RC slab upwards. However, the systems tested have some additional supports and bracing systems that can significantly affect the response of the chimney to lateral loading;
- Identification of resistance in terms of strength and displacement depending on the performance objectives;
- Structural identification of the system for future numerical modelling using Finite Element Method (FEM);
- Application of the obtained results to test the resistance of chimney systems to expected wind and earthquake loads.

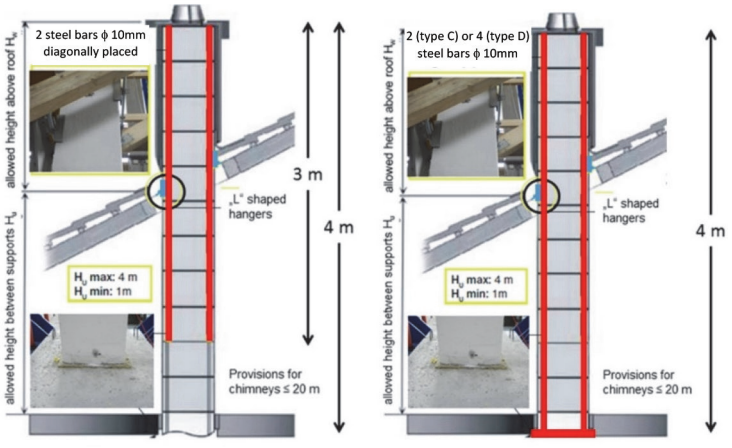

Figure 3. Boundary conditions of test setup, vertical section with longitudinal reinforcement bars trough the type A and B chimney systems (left) and for type C and D chimney system (right)

2.1 Experimental set-up

The chimneys were built in the laboratory conditions with the simulation of boundary conditions as close to the real application as possible. In the Figure 4, it is schematically shown the test setup of the chimney with all belonging supports and the actuator attached to the top of the chimney. The chimney was built with 12 lightweight concrete masonry units which all together with mortar between masonry blocks form a free-standing and cantilevered chimney with the total height of 3960 mm.

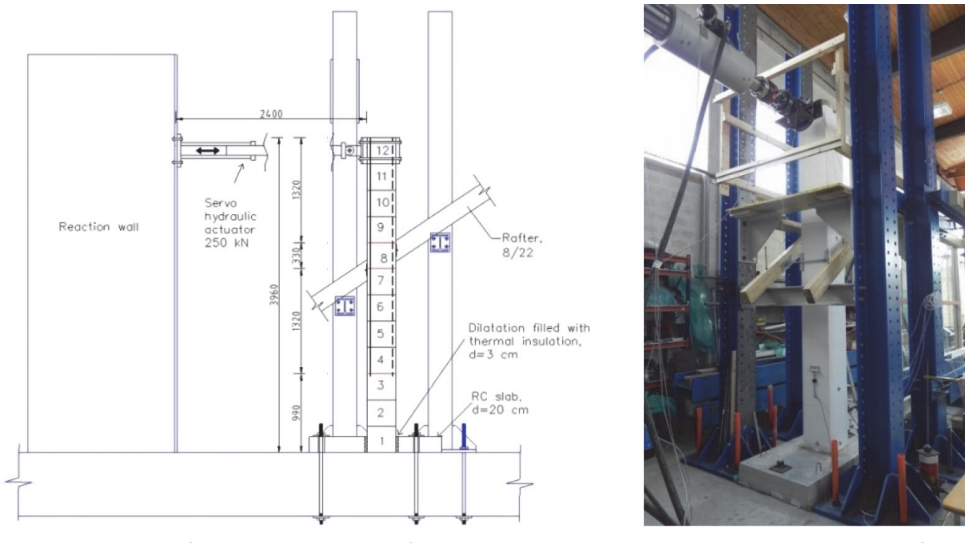

Figure 4. Test setup for laboratory testing of contemporary masonry chimney system with lateral force (left) and picture of test setup from laboratory prior testing

At the height of eight masonry chimney block the lateral bracing of the whole chimney was provided with "L" shaped hangers connected with two steel bars to the rafters on each side of the chimney. The lateral force to simulate the seismic load on tested chimneys was applied at the top masonry chimney block with the Instron (250 kN) servo-hydraulic actuator which was fixed with special clamping system on the chimney and at the other side to the reaction wall. The load was imposed through cyclic lateral displacements with stepwise increased amplitudes, repeated three times at each predefined displacement peak. To capture the chimneys behaviour all specimens were instrumented at particular positions with displacement transducers (LVDT-s) and accelerometers to measure displacements and frequencies respectively. In the Figure 5 positions of LVDT-s labelled with D1-8 and accelerometers labelled as A1-A6 are shown. Read arrow in the Figure 5 indicate the position and direction of lateral load application in relation to the measuring equipment. LVDT-s were placed to measure deformed shape along the height of the chimney in the direction of applied load. Whereas the accelerometers A1-A4 were mounted to capture the frequencies in the load direction along the height of the chimney once the cracks occurred and A5-A6 were placed perpendicular to the load direction at the top and bottom of the specimens.

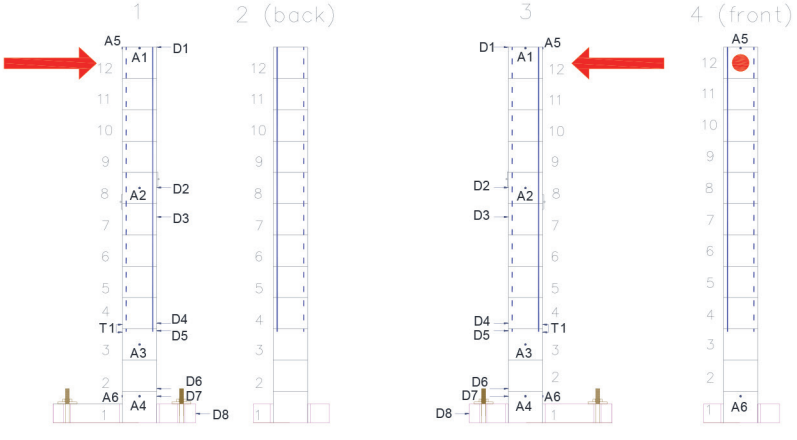

Figure 5. Positions of measuring equipment relative to the actuator. Read arrow shows the location and direction of lateral load application with the actuator

Measurement of dynamic characteristics were conducted with the procedure where the actuator was decoupled from the specimens at the top and then we pulled the chimney at the top with the force of 0,05 kN. After instant release of this force the accelerations were measured and analysed to obtain the time period T_s and damping ξ_s at different levels of specimen damage and programmed peak displacement at the top of the specimen.

2.2 Experimental results and main conclusions

All types of chimneys failed in flexure. The point of failure depends on the steel rebar position and length. Important element of tested chimney systems is also lateral bracing system at the roof level which provided effective elastic support for the whole chimney and allowed limited displacement and almost free rotation. Since greater flexural load bearing capacity was achieved for type C and D chimneys, higher load was activated on the lateral bracing system and consequently yielding of the lateral bracing system. Good cohesion between grout and masonry units was observed and no yielding of steel bars were observed following dismantling of the chimneys. Internal ceramic flue liners stayed intact during the tests.

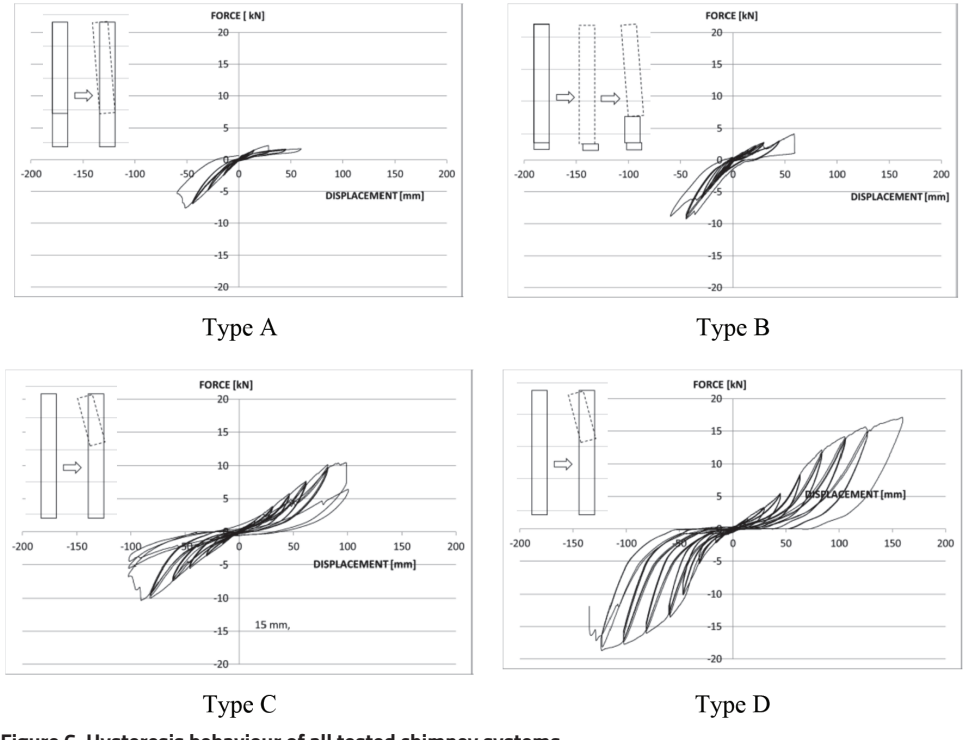

Figure 6. Hysteresis behaviour of all tested chimney systems

In the Figure 6 are shown the force-displacement hysteresis loops applied at the top of the specimens for all types of tested chimneys. It is apparent improvement of overall behaviour of chimney type C and D comparing to the initial version of chimney systems type A and B. It can be seen that for type A and B systems the resistance is significantly lower and asymmetrical. This phenomenon is a consequence of asymmetrical lateral bracing system and the formation of plastic hinge or damage at the beginning of reinforcement bars which is at the one-quarter height of the chimney. The location of plastic hinge formation and the critical damage is schematically shown in the Figure 6

beside the hysteresis diagram for each type of chimney system respectively. In negative direction, the lever arm is shorter and thus the stiffness as well as resistance was higher comparing to the positive direction. After the plastic hinge was formed, the chimney system turns into two kinematic bodies loosely attached with ceramic flue liners.
With extending the reinforcement bars along the whole height of the type C and D chimney systems, the crack pattern propagation and consequently failure mechanism changed. The chimney behaves as rigid body until the flexural and shear resistance of the chimney cross section at the contact with lateral bracing connected to the roof structure is exceeded. As soon as bracing system came into yielding phase, masonry units started cracking along the reinforcement bars and locally at the contact with the L shaped bracing system. The hysteresis behaviour of type C and D chimney systems show almost symmetrical response and greatly improved load bearing capacity which is more than 4 times higher comparing to the type A and B chimney systems. Moreover, the stiffness, ductility and dissipated energy is also improved with the reinforcement extension to the very bottom of the chimney systems C and D.
Left Figure 7 shows the formation of failure mechanism at the height where longitudinal steel reinforcement starts for type A and B chimney system. Whereas the right Figure 7 shows the formation of failure mechanism starting at the contact with the lateral bracing system at the roof structure level for type C and D chimney systems.

Figure 7. Identified resisting system and typical damage patterns for type A and B (left) and for type C and D (right)

Following dynamic tests carried out before and after the main cyclic tests, Fast Fourier Transformation (FFT) analysis of the recorded signals from the top two accelerometers (A1 and A5) in both directions was performed to obtain the chimneys dynamic characteristics. Based on this analysis we were able to evaluate the natural time period T_s and damping ξ_s of chimney systems at different level of chimney damage. The results are shown in the Table 2 and Table 3 for the chimney type A, B and type C, D respectively.

For further analysis and definition of floor acceleration spectra for chimneys the results of frequency analysis at the initial and laterally braced system is important and we can see that the time period of type D chimney is significantly lower in comparison to the others. This again proves that this chimney system is the stiffest and corresponds the fact that is reinforced along the whole height and in all four corners and that the cross section is slightly bigger. The initial damping was as expected relatively high. After the applied load the damage of the chimneys occurred which corresponds to the increasing damping and time period.

Table 1. Damping ξ_s and period T_s for type A and B chimney systems at different levels of applied displacement

	Type A				Type B			
	A1		A5		A1		A5	
	ξ_s [%]	T_s [s]	ξ_s [%]	T_s [s]	ξ_s [%]	T_s [s]	ξ_s [%]	T_s [s]
Initial, braced	7,3	0,102	5,9	0,102	3,0	0,081	4,4	0,082
d = 15 mm	8,0	0,205	12,2	0,205	5,5	-	3,7	-
d = 30 mm	12,1	0,205	14,1	0,410	8,5	0,137	5,5	0,205
d = 45 mm	-	-	-	-	9,8	0,145	12,3	0,205

Table 2. Damping ξ_s and period T_s for type C and D chimney systems at different levels of applied displacement

	Type C				Type D			
	A1		A5		A1		A5	
	ξ_s [%]	T_s [s]	ξ_s [%]	T_s [s]	ξ_s [%]	T_s [s]	ξ_s [%]	T_s [s]
Initial, braced	10,1	0,090	12,58	0,091	4,65	0,068	7,20	0,068
d=60 mm	12,2	0,130	15,14	0,133	-	-	-	-
d=100 mm	-	0,101	-	0,105	6,02	0,117	11,15	0,117
d=120 mm or end	-	0,137	-	0,145	-	0,117	-	0,117

3. Seismic load on chimney system for typical single family house

As required by the new European building codes (Eurocodes) proposal prEN 1998-1-2:2019.3 (E) [4] we have generated floor acceleration spectra with the simplified method developed by the authors Vukobratović and Fajfar recently and is in more detail presented in [8], [9], [10]. Common detached single family house presented in the Figure 8 was taken as a case study. The house architecture and approximate dimensions were taken from typical houses catalogue [11] and has ground floor, attic floor above with sloping roof and contemporary masonry chimney with the same proportions and dimensions as those tested in our laboratory and presented in section 2.

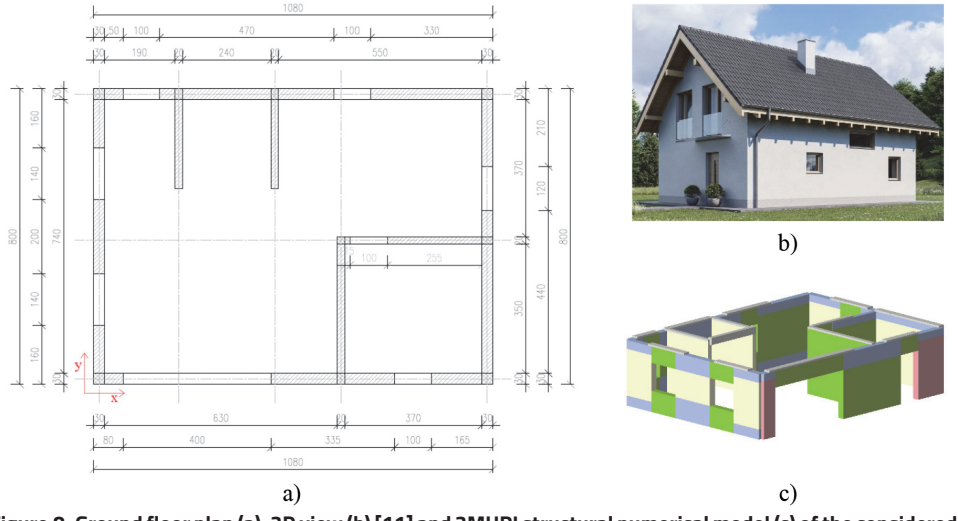

Figure 8. Ground floor plan (a), 3D view (b) [11] and 3MURI structural numerical model (c) of the considered typical detached family house

For comparison we evaluated the first floor acceleration spectra where elastic primary structure $A_{e,s,1}$ and inelastic primary structure $A_{s,1}$ behaviour were considered. The secondary structure was considered as elastic structure. In the Figure 9 the first floor acceleration spectra for elastic and inelastic primary structure is shown in addition to the elastic ground response spectrum. These floor response spectra are determined with the SRSS modal combination rule of the floor acceleration spectra for the first three individual modes. The obtained floor acceleration spectra for the elastic and inelastic primary structure is almost the same for the whole time period range. The difference is at the peak values at the resonance region where considering the inelastic primary structure behaviour decrease the peak acceleration value down to 2,45g from 2,8g for elastic primary structure.

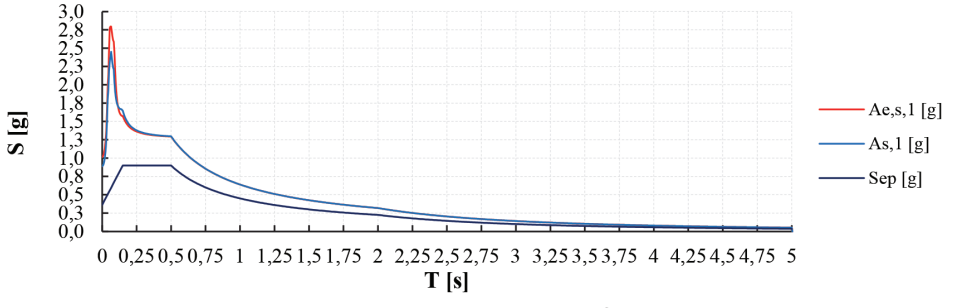

Figure 9. Floor acceleration spectra $A_{e,s,1}$ where elastic behaviour of structure is considered and $A_{s,1}$ where inelastic behaviour of primary structure is considered. S_{ep} represents elastic ground response spectrum

Based on the experimentally obtained natural periods T_s for four tested types of contemporary masonry chimneys for the initial state (uncracked) and for the state after the first crack appeared, represented in Table 2 and Table 3 we evaluated the accelerations $A_{e,s,1}$ and $A_{s,1}$ represented in the Figure 9 acting on the chimneys. The results are shown in Table 4 where the floor accelerations $A_{e,s,1}$ and $A_{s,1}$, masses m of chimney systems and corresponding activated lateral force $F_{e,s,1}$ and $F_{s,1}$ acting in the centre of chimney mass. Note that the $F_{e,s,1}$ and $F_{s,1}$ correspond to the elastic and inelastic primary structure behaviour correspondingly. As expected the seismic forces for the improved chimney type D with reinforcement in all four corners along the whole height were the highest and amounted up to 10 kN and drop substantially upon cracking of chimney. Meanwhile the acting forces on chimney type A and B are the lowest. The forces $F_{e,s,1}$ and $F_{s,1}$ represented here in Table 4 are actually forces acting on the L-shaped lateral support braces connecting the chimney and roof structure. There was no damage recorded up to applied force of 10 kN during the test conduction at the lateral chimney support which means that this bracing system behave adequately for the earthquake scenario presented in Table 4. In the last column of Table 4 the approximate lateral force $F_{s,1,top}$ acting at the top of the chimney, corresponding to the experimental one, is presented. It is calculated based on the condition that this force $F_{s,1,top}$ generate the reaction force at the roof structure lateral support level equal to the force $F_{s,1}$ induced by the inelastic floor acceleration spectra. It is found that the seismic load on chimney and lateral bracing support is way below those obtained during the experiment conduction for type C and D chimneys where at the applied force 10,33 kN and 14,12 kN damage limitation state was achieved correspondingly. Meanwhile the damage limitation state for type A and B chimney systems was achieved during the experiment when the forces of 2,27 kN and 2,34 kN were applied correspondingly. This implicate that the seismic forces evaluated at the top of the chimney in our case study exceed that limit substantially which means that some serious damage could occur at the level where the reinforcement start at one third of the chimney height.

Table 3. Seismic lateral load ($F_{e,s,1}$, $F_{s,1}$, $F_{s,1,top}$) on different chimney types evaluated based on floor acceleration spectra acting in the centre of chimney mass and at the top of the chimney

	Tip dimnika	$A_{e,s,1}$ [g]	$A_{s,1}$ [g]	m [kg]	$F_{e,s,1}$ [kN]	$F_{s,1}$ [kN]	$F_{s,1,top}$ [kN]
Initial state	A	1.9	1.8	316	5.9	5.6	3.7
	B	2.6	2.23	296	7.5	6.5	4.2
	C	2.44	2.03	316	7.6	6.3	4.1
	D	2.74	2.4	372	10.0	8.8	5.7
First crack	A	1.41	1.44	316	4.4	4.5	2.9
	B	1.58	1.66	296	4.6	4.8	3.2
	C	1.61	1.67	316	5.0	5.2	3.4
	D	1.7	1.7	372	6.2	6.2	4.1

4 Conclusions

The behaviour of four different types of contemporary masonry chimney systems were tested under lateral load. The reinforcement in the first two types was placed in two diagonal corners and only along the upper three quarters of the chimney height. This system provokes the plastic hinge of the chimney where the reinforcement starts at one quarter of the chimney height. The presence of continuous rebar along the whole height of the second two tested chimney systems proved superior behaviour as the extension of reinforcement significantly improve load bearing capacity and stiffness of the whole system. The presence of continuous reinforcement prevented the formation of plastic hinge at the beginning of reinforcement. Additionally, in the last tested chimney system, the reinforcement was inserted in all four corners along the whole height of the specimen, which additionally prevented torsional effect due to the asymmetrical reinforcement. Failure of improved system with continuous reinforcement occurred at the height of bracing system at the roof structure level due to the failure of masonry units along the reinforcement. Bracing system acted as an effective element for all four chimney systems and only in case of continuous reinforcement the bracing system was activated to the yielding level. In the end we also performed the calculation of seismic forces acting on the chimney built into a typical modern detached family house with attic so that the proportions and dimensions of chimney above the first floor slab were the same as those in conducted experiment. Based on the experimental results and determined floor response spectra of first floor we evaluated the seismic force acting in the centre of chimney mass which is approximate acting force on the lateral bracing support at the roof level. It was found that the seismic load on chimney and lateral bracing support is way below those obtained during the experiment conduction for type C and D chimneys, whereas for type A and B system the load bearing capacity is exceeded and damage limitation state may be reached.

Acknowledgements

The presented research work was conducted within the applicative project financed by industrial partner Schiedel Gmbh Austria and partly cofounded by the Slovenian Research Agency through research programme P2-0185.

References

[1] Simicevic, V.,: *Climbers, cavers, high-rise workers help clean debris from rooftops after Zagreb earthquake*, Alpinist Magazine, Vermont, http://www.alpinist.com/, Version: 28.4.2020, http://www.alpinist.com/doc/web20s/newswire-climbers-help-after-zabgreb-earthquake, (accessed 12th February 2021).

[2] Osteraas, J., Krawinkler, H., (2010): FEMA P-58/BD-3.9.7 Background Document, Fragility of Masonry Chimneys, December, *U.S. Department of Homeland Security*.

[3] Snoj, J. (2014): Seismic risk assessment of masonry buildings, PhD Thesis, *University of Ljubljana*, Slovenia, September.

[4] prEN 1998-1-2:2019.3, (2003): Eurocode 8: Design of structures for earthquake resistance - Part 1-2: Rules for new buildings; *CEN/TC 250*, Brussels, Belgium.

[5] EN 1998-6, (2005). Eurocode 8: Design of structures for earthquake resistance - Part 6: Towers, masts and chimneys; *CEN*, Brussels, Belgium., June

[6] Bosiljkov, V., Antolinc, D., Steinecker, G., Plaskan, S. (2016): Experimental research on the seismic behaviour of contemporary masonry chimney systems, *Procedings of the 16th International Brick and Block Masonry Conference*, Padova, Italy, pp. 2371-2379.

[7] Bosiljkov, V., Antolinc, D., Steinecker, G., Plaskan, S. (2018): Optimization of the seismic performance of contemporary masonry chimney systems, *Procedings of 10th Australian Masonry Conference*, Sydney, Australia, 12 pages.

[8] Vukobratović, V., Fajfar, P., (2015). A method for the direct determination of approximate floor response spectra for SDOF inelastic structures, *Bull Earthquake Eng* 13:1405–1424, DOI 10.1007/s10518-014-9667-0

[9] Vukobratović, V., Fajfar, P., (2016). A method for the direct estimation of floor acceleration spectra for elastic and inelastic MDOF structures, *Earthquake Engineering and Structural Dynamics* 45:2495-2511, DOI 10.1002/eqe.2779

[10] Vukobratović, V., Fajfar, P., (2017). Code oriented floor acceleration spectra for building structures, *Bull Earthquake Eng* 15:3013-3026, DOI 10.1007/s10518-016-0076-4

[11] Ytong hiše, Slovenia, https://www.ytonghisa.si/nizkoenergijske-hise/?h=manca-122-m2, (accessed 8th February 2021).

[12] EN 1996-1, (2005). Eurocde 6 – Part 1-1: General rules for reinforced and unreinforced masonry structures, *CEN*, Brussels, Belgium. June